A&A manuscript no.
(will be inserted by hand later)

Your thesaurus codes are:
03(11.17.1; 11.05.2; 11.09.3)

ASTRONOMY
AND
ASTROPHYSICS
1.2.2008

Observational constraints on the nature of low redshift Lyα absorbers*

V. Le Brun[1], **J. Bergeron**[2,1], **and P. Boissé**[3]

[1] Institut d'Astrophysique de Paris, CNRS, 98bis boulevard Arago, F-75014 Paris, France
[2] European Southern Observatory, Karl-Schwarzschild Straße 2, D-85748 Garching, Germany
[3] Ecole Normale Supérieure, 24 rue Lhomond, F-75005 Paris, France

Received 13 January, accepted 6 June 1995

Abstract. We present results from a spectroscopic and imaging survey of galaxies in the fields of quasars from the Hubble Space Telescope (HST) Quasar Absorption Line Key Project. The aim of this survey is to identify galaxies within 3.5′ from the quasar sightline, to a limiting, integrated r-band magnitude $m_{\rm r} = 22.5$. The data are then compared to the HST homogeneous sample of Lyα-only absorbers in order to put constraints on the nature of these absorbers, and in particular on their relation to galaxies.

We have obtained spectra for 81 objects in three quasar fields and identified 66 galaxies (success rate of 81%) at redshifts in the range $z = 0.0500$-0.7974, and at linear impact parameters to the quasar sightlines spanning D=57-2380 h_{50}^{-1} kpc. Among these galaxies, 19 are at less than 750 km s^{-1} from a Lyα absorber, and only one clearly does not give rise to any absorption. Three other galaxies are at the redshifts of metal-rich absorption systems, of which one belongs to a cluster with altogether 19 identified galaxies at the quasar redshift.

The analysis of our sample combined with those of previous studies shows that:

1) the redshift agreements of the Lyα absorber-galaxy associations cannot be due to chance coincidence;

2) there is no clear anti-correlation between the Lyα rest-frame equivalent width and the impact parameter for the whole sample ($w_{\rm r,min}$=0.10 Å). When only the strongest lines are considered ($w_{\rm r} \geq 0.24$ Å), $w_{\rm r}$ (Lyα) and D are marginally anti-correlated. Lanzetta et al. (1995) found a stronger anti-correlation which could be due, at least in part, to the existence of metal-rich absorbers in their sample. Our results suggest that most Lyα absorbers are not gaseous clouds that belong in a strict sense to galaxies, as is the case for Mg II absorbers. The size of Lyα galactic halos can be inferred from the variation with D of the fraction of associations to the total number of galaxies at impact parameters $< D$. This fraction drops from 1 to ~ 0.65 at $D \sim 200 h_{50}^{-1}$ kpc and flattens at larger values of D ($\gtrsim 300 h_{50}^{-1}$ kpc). This leads to Lyα galactic halos sizes about three times larger than the inner Mg II halo region;

3) there is no correlation between the galaxy luminosity and the impact parameter. This again suggests that a significant Lyα clouds do not belong to individual galaxies, but instead are distributed in the local large-scale structure. For the smaller impact parameters, this could reflect a link between D and the total galaxy mass rather than its luminous mass;

4) the HWHM=120 km s^{-1} of the relative velocity distribution of the Lyα absorber-galaxy associations is consistent with either galaxy rotation velocities or the local velocity dispersion in large-scale structures.

Key words: quasars: absorption lines – Galaxies: evolution – intergalactic medium

Send offprint requests to: V. Le Brun

* Based on observations made at the Canada-France-Hawaii-Telescope, Hawaii, USA

1. Introduction

The homogeneous samples of Lyα and C IV absorption lines detected in quasar spectra observed with the Hubble Space Telescope (HST) are of primary importance to investigate the properties of the intergalactic medium and the gaseous content of galaxies at low redshift. These UV spectra when combined with ground-based observations of higher redshift absorption lines, provide a data base which allows to determine the evolution in cosmic time of gaseous objects covering a very large range in H I column density.

Analysis of the results from the HST absorption line survey (Bahcall et al. 1991, 1993, 1994) shows that the "Lyα absorbers" (with absorption lines only from the Lyman series) constitute the dominant population at all redshifts and that their number density at low redshift is somewhat higher than expected from an extrapolation of the data obtained in the range $1.7 < z < 3.5$ (Bahcall et al. 1993, 1994). Groups of Lyα lines are found close in redshift to about half of the extensive metal-line systems (Bahcall et al. 1994).

From a study of the Lyα absorber-galaxy correlation function, Morris et al. (1993) have suggested that all galaxies more luminous than 0.1 $L^\star$ have effective cross-sections of 0.5-1 h_{50}^{-1} Mpc, where h_{50} is the Hubble constant in units of 50 km s^{-1} Mpc^{-1} and the deceleration parameter is assumed to be equal to zero. This however does not imply a physical association between the Lyα absorbers and individual galaxies. Lanzetta et al. (1995, hereafter LBTW) have found an anti-correlation between the impact parameter of the absorption-line selected galaxies and the rest equivalent width of the Lyα absorption line which suggests a tight physical link between absorbers and galaxies. These authors conclude that most luminous galaxies are surrounded by extended galactic halos of radius $r \sim 345 h_{50}^{-1}$ kpc (using $q_0 = 0$ and $z = 0.3$). Recently, Morris & van den Bergh (1994) have proposed that tidal effects may play an important role in extracting gas from the disc of galaxies and spreading it over hundreds of kiloparsecs. It is indeed likely that at least some of the Lyα systems are caused by tidal debris which remain loosely associated with the parent galaxies (assuming that the gas is leaving the galaxy with a velocity of 100 km s^{-1} in excess of the escape velocity, the expected linear separation after 3×10^9 yr is about $300 h_{50}^{-1}$ kpc). In this picture, the intervening gas is supposed to be "physically associated" to the galaxy, in the sense that it originated from it. However, for large impact parameters, the link between Lyα absorbers and galaxies could be only apparent if the Lyα absorptions were due to gaseous clouds distributed in space in the same way as dark matter (Cen et al. 1994; Petitjean et al. 1995). Such a situation could result from a partial inefficiency in the galaxy formation process that would have left clumps of metal-poor gas displaying the same large-scale distribution as galaxies.

As at high redshift, the C IV systems are the dominant population of metal-rich absorbers at $z_a \sim 0.5$ (Bahcall et al. 1993) and often show associated O VI absorption (Lu & Savage 1993; Bahcall et al. 1993, 1994). Over the redshift range $z \simeq 0.15$-1.05, Mg II absorption systems have been identified with large gaseous halos around bright ($-24 < M_r < -20$) galaxies (Bergeron & Boissé 1991 and references therein; Bergeron et al. 1992; Steidel 1993). There is a correlation between the radius of these Mg II halos and the galaxy luminosity, $R \simeq 75 (L/L^\star)^\alpha h_{50}^{-1}$ kpc, where $\alpha \simeq 0.2$ to 0.3 (Bergeron & Boissé 1991; Le Brun et al. 1993; Steidel 1993). The linear scales probed by Mg II absorbers is thus much smaller than those typical for Lyα absorbers. Few C IV absorption systems have been so far identified, but they most probably arise in extended galactic halos of size similar to those of Mg II absorbers or possibly slightly larger. One of the Mg II-absorption selected galaxy has associated C IV and O VI absorptions (Bergeron et al. 1994), and two other C IV systems have recently been identified by LBTW. The impact parameters of these three C IV-absorption selected galaxies cover the range $d = (58\text{-}95) h_{50}^{-1}$ kpc. The high ionization O VI absorbers could be an homogeneous phase of low density and large extent in which C IV and Mg II clouds are embedded. Galactic halos around bright galaxies are a common phenomenon at moderate redshift and their most outer parts might only be probed by Lyα absorbers.

The identification of a large sample of low redshift Lyα systems is needed to investigate in more details the nature of these absorbers and determine which fraction of them correspond to gas that is truly associated with galaxies. To this aim, we have undertaken a spectroscopic survey of galaxies around quasars of the HST Key Project. The study of three fields, reported in this paper, substantially increases the size of the sample of galaxies in the environment of Lyα absorbers. We have searched for possible correlations involving the impact parameter of the galaxy, its luminosity, the Lyα absorber-galaxy velocity difference and the equivalent width of the Lyα absorption line in order to constrain the nature of Lyα absorbers: gravitationally bound very extended galactic halos, gas extracted by tidal interaction or intergalactic gas that traces the distribution of luminous and dark matter in the universe.

The observations and data reduction are presented in Sect. 2. The list of identified galaxies and the description of individual fields are given in Sect. 3. Results of statistical analyses of the combined sample, which includes studies from other groups, are presented in Sect. 4. In Sect. 5, we discuss the implications of these results on the nature of the Lyα absorbers and present our conclusions.

2. Observations and data reduction

The log of the observations is given in Table 1.

Table 1. Journal of the observations

Object	Dates	Instrument	mode	Filter or Grism	n $\times\Delta t$ mn
Ton 153	1992 March, 27	FOCAM	Imaging	r	3×7
	1993 May 18,20,21	MOS-SIS	Imaging	r	5×5
	1993 May 20,21	MOS-SIS	Multi Spect.	O 300	3×90
3C 351	1992 March, 27	FOCAM	Imaging	r	4×5
	1993 May 17,19	MOS-SIS	Imaging	r	3×5[a]
	1993 May 19	MOS-SIS	Multi Spect.	O 300	2×90
H 1821+6419	1992 Sept 28	HRCAM	Imaging	r	3×10
	1993 May 16,17,18	MOS-SIS	Imaging	r	3×5[a]
	1993 May 17,18	MOS-SIS	Multi Spect.	O 300	3×90

[a] Only two exposures were used to obtain the final image due to a displacement of the CCD on the 18^{th}.

2.1. Imaging

The images were obtained at the prime focus of the CFH Telescope with the Faint Object Camera (FOCAM) or the High Resolution Camera (HRCAM). The CCD is a 640×1024 pixel RCA with a plate scale of $0.2055''$ per pixel for FOCAM and a 1080×1080 pixel SAIC with a plate scale of $0.1311''$ per pixel for HRCAM. The ESO software package MIDAS was used at all steps of the data processing. The images were reduced in a standard way, with subtraction of individual overscan and of a median filtered bias before flat-fielding. The flat-field was obtained by an averaging procedure including pixel rejection, applied to all the images (at least 16) with a similar background level. The resulting image was then normalized. A shift-and-add procedure was used, and the averaging obtained with a median filter allowed a successful removal of cosmic ray events.

Other images were taken with the CFHT Multi-Object Spectrograph (MOS) in the imaging mode. The CCD is a $(2048)^2$ pixel Lick 3 with a plate scale of $0.3140''$ per pixel. The actual field imaged is $9.7'\times 9.4'$. The same reduction procedures have been applied; in addition, a distortion map was used to correct for the optical distortion which is fairly strong in the field corners. Due to this optical distortion and the poorer sampling of MOS, the images obtained with this instrument are only used to study the galaxies further away to the quasar line of sight, the closest ones being better investigated with the higher-quality FOCAM/HRCAM images.

Table 2. Galaxy population of the fields

	TON 153			3C 351			H 1821+6419		
Magnitude range	N_{gal}^{a}	N_z^{b}	Comp.[c]	N_{gal}^{a}	$N_z^{b,d}$	Comp.[c]	N_{gal}^{a}	$N_z^{b,e}$	Comp.[c]
$m_r \leq 17.5$	1	0	0%	4	1 (+2)	75%	1	1 (+0)	100%
$17.5 < m_r \leq 18.5$	2	2	67%	4	2 (+2)	87%	6	1 (+1)	43%
$18.5 < m_r \leq 19.5$	1	0	40%	4	2 (+0)	75%	30	7 (+5)	40%
$19.5 < m_r \leq 20.5$	9	2	31%	9	1 (+1)	52%	67	6 (+1)	21%
$20.5 < m_r \leq 21.5$	25	9	34%	54	4 (+1)	21%	124	3 (+1)	11%
$21.5 < m_r \leq 22.5$	58	5	19%	120	5 (+0)	11%	158	0 (+0)	7%

[a] N_{gal} is the number of galaxies in each magnitude bin within $3.5'$ of the quasar sightline

[b] N_z is the number of galaxies in each magnitude bin with measured redshift

[c] Completeness, it refers to the cumulated distribution of magnitudes

[d] The additional numbers in brackets show the redshifts obtained by LBTW

[e] The additional numbers in brackets show the redshifts obtained by Schneider et al. (1992)

2.2. Spectroscopy

Galaxy spectra have been obtained with MOS in the multi-slit spectroscopy mode. We have observed between 25 and 28 galaxies per mask with slitlets of 15 to 18″ length and 1.5″ width. After correction of the distortion, overscan and bias subtraction, the spectra have been divided by an averaged dome flat-field. The grating used gives a useful, maximum wavelength range of $4400 \leqq \lambda \leqq 9700$ Å, a wavelength dispersion of 3.6 Å per pixel and a resolution of FWHM = 18 Å for a 1.5″ slit-width. The wavelength calibration was done using Helium and Argon spectra. Spectra of standard stars were taken in one of the slitlets of different masks for flux calibration. Thereafter, we have developed semi-automatic procedures to reduce the multiple spectra. For the wavelength calibration, identification of only one set of He or Ar lines is needed for a given mask, e.g. in the first slitlet, the recognition being then made automatically in each of the other slitlets. For individual exposures of a given field, the sky is fitted along the spatial rows by a polynomial of low order, after a strong filtering to avoid spurious features due to cosmic ray events. The extraction of the spectra is done with a weighted average of the spatial rows. The cosmic ray hits, present on the galaxy spectra themselves, are removed by comparing the spectra obtained from different exposures.

The redshifts have been measured using strong emission and absorption lines, when present. For the other galaxies, the cross-correlation task "xcsao" of IRAF has been used. We have determined 66 definite galaxy redshifts for the three fields, thus a success rate of 81%.

3. Identification of the galaxies and description of the individual fields

To search for galaxies (possibly) related to Lyα absorbers, we first need to define a criterion involving the relative velocity between the absorbers and the galaxies, Δv. Let us first discuss the maximum absolute value of Δv which would be appropriate to associate gas to a given galaxy. For ellipticals, the average velocity dispersion is about 200 km s^{-1}, and can reach 300 km s^{-1}; the rotational velocity is smaller and its maximum value is around 150 km s^{-1} (de Zeeuw & Franx 1991). The radial velocity in spirals is correlated to the galaxy luminosity. In normal galaxies, the velocity at large radii is of the order of 200-250 km s^{-1}, and can reach 350 km s^{-1} for the most luminous galaxies (Rubin et al. 1982). In starburst-driven galactic superwinds, the total velocity variation along extended emission-line region is of order 600 km s^{-1}, and in some cases is as large as 900 km s^{-1} (Heckman et al. 1990). Within large-scale structures, the typical velocity spread between galaxies within a sheet-like structure is about 500 km s^{-1}, and may reach 750 km s^{-1} (Ramella et al. 1989). Given the uncertainties in the redshift measurements of both the Lyα absorption lines and the field galaxies, $|\Delta z| \leq 0.0003$ for our sample as well as for that of Morris et al. (1993) and LBTW, we have adopted as maximum, relative velocity between the Lyα absorber and the "associated galaxy" $|\Delta v| = 750$ km s^{-1}.

For comparison, the largest values of $|\Delta v|$ in the sample of Morris et al. (1993) is 710 km s^{-1} and the relative velocity criterion adopted by LBTW is $|\Delta v| < 1000$ km s^{-1} to include absorber-galaxy associations on scales up to those of clusters of galaxies. In the LBTW GA sample, restricted to unambiguous redshift identifications, the largest value of $|\Delta v|$ is just below 500 km s^{-1}.

The total number of galaxies within 3.5′ of a quasar sightline in the different magnitude bins, the number of galaxies with measured redshifts and the completeness for the cumulative galaxy distribution are given in Table 2 for the three quasar fields. The redshifts, magnitudes and distances (Δx=$-\Delta\alpha$, Δy=$\Delta\delta$) to the quasar sightlines of the galaxies with spectroscopic data are listed in Tables 3, 4 and 5 for the fields around TON 153, 3C 351 and H 1821+6419, respectively. The Lyα system(s) within 750 km s^{-1} of the galaxy redshift are listed in Column 7, and the comments given in Column 8 refer to the nature of the absorption system, atmospheric features in the quasar spectra occuring at the expected wavelength of the Lyα absorption possibly associated with the galaxy or the lack of available data at the galaxy redshift.

3.1. The field toward TON 153 ($z_{\rm em}$=1.022)

There are 36 Lyα-only absorption systems detected in the HST spectrum of TON 153 (Bahcall et al. 1994). One system is at the quasar redshift and shows associated O VI absorption. There are two other metal-rich systems, one with only C IV absorption at $z_{\rm a} = 0.2891$ and a very strong system at $z_{\rm a} = 0.6606$ with Lyα, Lyβ, C II, C III, Si II and Si III absorption lines. For the 28 objects in this field with spectroscopic data, we have obtained 23 redshift identifications, one of the objects being a star (Table 3). The field around TON 153 is shown in Fig. 1, in which the studied objects are encircled by the slitlet contours. Among the 22 identified galaxies, seven have one or more associated Lyα-only system from the list published by Bahcall et al. (1994). There is a clump of five Lyα absorption lines covering an interval of 1400 km s^{-1} and centred at $z_{\rm a} = 0.673$. The metal-rich system, at $z_{\rm a} = 0.6606$, is within 1600 km s^{-1} of the nearest member of the Lyα-only clump (Bahcall et al. 1994). Three galaxies at $z_{\rm g} \simeq 0.67$ are clustered in velocity space over 1400 km s^{-1} and, together with the galaxy in the slitlet #25 ($z_{\rm g} = 0.6639$), fall within a projected area

Table 3. Characteristics of the TON 153 field

Gal	Δx($''$)	Δy($''$)	θ($''$)	d(kpc)	$z_{\rm g}$	$z_{\rm a}$	Observations	$m_{\rm r}$	$M_{\rm r}$
QSO	0.0	0.0	0.0	0.0	1.0220			16.0	-28.9
1	267.4	19.5	268.1	920.3	0.1442		unobs.[a]	19.9	-19.9
2	255.3	-28.4	256.8	1263.1	0.2291		unobs.[a]	19.3	-21.7
3	232.0	25.4	233.4	2013.7	0.5674		Coinc.[b]	21.5	-21.7
4	208.9	-118.7	240.3	2375.7	0.7663	0.7667	Lyα	22.7	-21.3
5	192.2	29.3	194.4	1624.0	0.5324	0.5349	Lyα	21.7	-21.3
6	176.0	-3.3	176.0	1669.7	0.6952	0.6947	Lyα (Bl.[c])	21.8	-22.0
7	163.8	23.5	165.5	223.9	0.0500		unobs.[a]	18.4	-19.0
8	142.5	-91.1	169.1	423.3	0.0992		unobs.[a]	21.0	-18.0
9	118.7	-26.1	121.5	770.1	0.3310		unobs.[a]	19.7	-22.1
10	99.7	-41.4	107.9	766.2	0.3976		Coinc.[d]	22.2	-20.1
12	78.9	-69.2	105.0	996.9	0.6974	0.6958	Lyα (Bl.[c])	22.3	-21.4
13	56.9	-78.3	96.8	634.5	0.349		unobs.[a]	20.6	-21.3
14	42.4	-62.6	75.6	438.1	0.2891	0.2891	metal	20.4	-21.1
15	19.8	-108.4	110.1	472.6	0.1910		unobs.[a]	18.0	-22.5
16	6.8	4.8	8.3	77.5	0.6715	0.6716, 0.6736	Lyα	21.7	-22.0
17	-10.9	-7.8	13.4		indef.			23.0	
18	-25.6	-96.4	99.7		0.0000		star	21.3	
19	-44.4	-2.3	44.5	415.3	0.6717	0.6716, 0.6736	Lyα	22.3	-21.3
20a	-66.1	10.5	67.0	563.5	0.5397	0.5436	Lyα (Bl.[e])	20.8	-22.3
20b	-68.1	9.7	68.7	578.4	0.5398	0.5436	Lyα (Bl.[e])	21.1	-22.0
21	-82.3	32.6	88.5		indef.			21.3	
22	-96.9	25.7	100.3		indef.			22.8	
23	-114.5	-107.4	157.0	1421.1	0.6265	0.6267	Lyα (Bl.[f])	20.7	-22.8
24	-129.5	-31.5	133.3	1242.4	0.668	0.6692	Lyα	20.5	-23.2
25	-155.6	-29.1	158.3	1471.1	0.6639	0.6606	metal	21.3	-22.4
26	-170.2	6.6	170.3	739.9	0.1944		unobs.[a]	20.5	-20.0
27	-194.4	13.4	194.8		indef.			20.7	
28	-213.5	-23.3	214.8		indef.			22.4	

[a] At these redshifts, there are no available HST data on Lyα absorption.
[b] The Lyβ line at 1902.02 Å is at less than 750 km s^{-1} from the galaxy redshift (see text).
[c] These two absorption redshifts come from a two-component fit to the Lyα line at 2060.88 Å (see text).
[d] The very strong Lyβ line at $z_{\rm a} = 0.6606$ is at 1703.30 Å whereas Lyα at the galaxy redshift is expected at 1699.02 Å (see text), that is 750 km s^{-1}.
[e] Same as [c] but for the Lyα line at $z_{\rm a} = 0.5454$ (see text).
[f] Same as [c] but for the Si II(λ1190.42) line at $z_{\rm a} = 0.6606$ (see text).

of $1.5 \times 0.3 h_{50}^{-2}$ Mpc^2. Object # 25 is most probably not responsible for the strong metal-rich system, given its large impact parameter ($l = 1420 h_{50}^{-1}$ kpc). Since we do not have a complete, magnitude limited sample, it is likely that the $z = 0.6606$ absorber is to be found among the galaxies close to the quasar sightline which have not been investigated spectroscopically. The same comment applies to the galaxy in slitlet #14, which is exactly at the redshift of the $z_{\rm a} = 0.2891$ C IV absorption system, but at a large impact parameter, $440 h_{50}^{-1}$ kpc.

Two Lyα systems are at less than 750 km s^{-1} of each of the two galaxies #16 and #19. For the closest to the quasar sightline, we have assigned the closest system in redshift space.

Two galaxies (# 6 and # 12) can a priori be assigned to the same Lyα absorption line at $z_{\rm a} = 0.6952$, but this line is clearly a blend of two components, at $z_{\rm a} = 0.6947$ and 0.6958. Each of them has thus been assigned to the galaxy with the closest redshift.

For three other galaxies(#20a, #20b and #23), there is no associated Lyα absorption in the published lists. We thus checked for possible Lyα absorption at a detection limit less than 4.5σ. The pair of interacting galaxies in the slitlet # 20, $570 h_{50}^{-1}$ kpc away on the sky from the quasar image, and at $z_{\rm g} = 0.5397$, is at about 1000 km s^{-1} from the $z_{\rm a} = 0.5454$ Lyα system. A closer look at the $z_{\rm a} = 0.5454$ Lyα absorption line clearly reveals two components, one at $\lambda = 1878.32$ Å and the second at $\lambda = 1876.48$ Å. This second line corresponds to a Lyα absorption at $z_{\rm a} = 0.5436$, or 750 km s^{-1} from the galaxy pair.

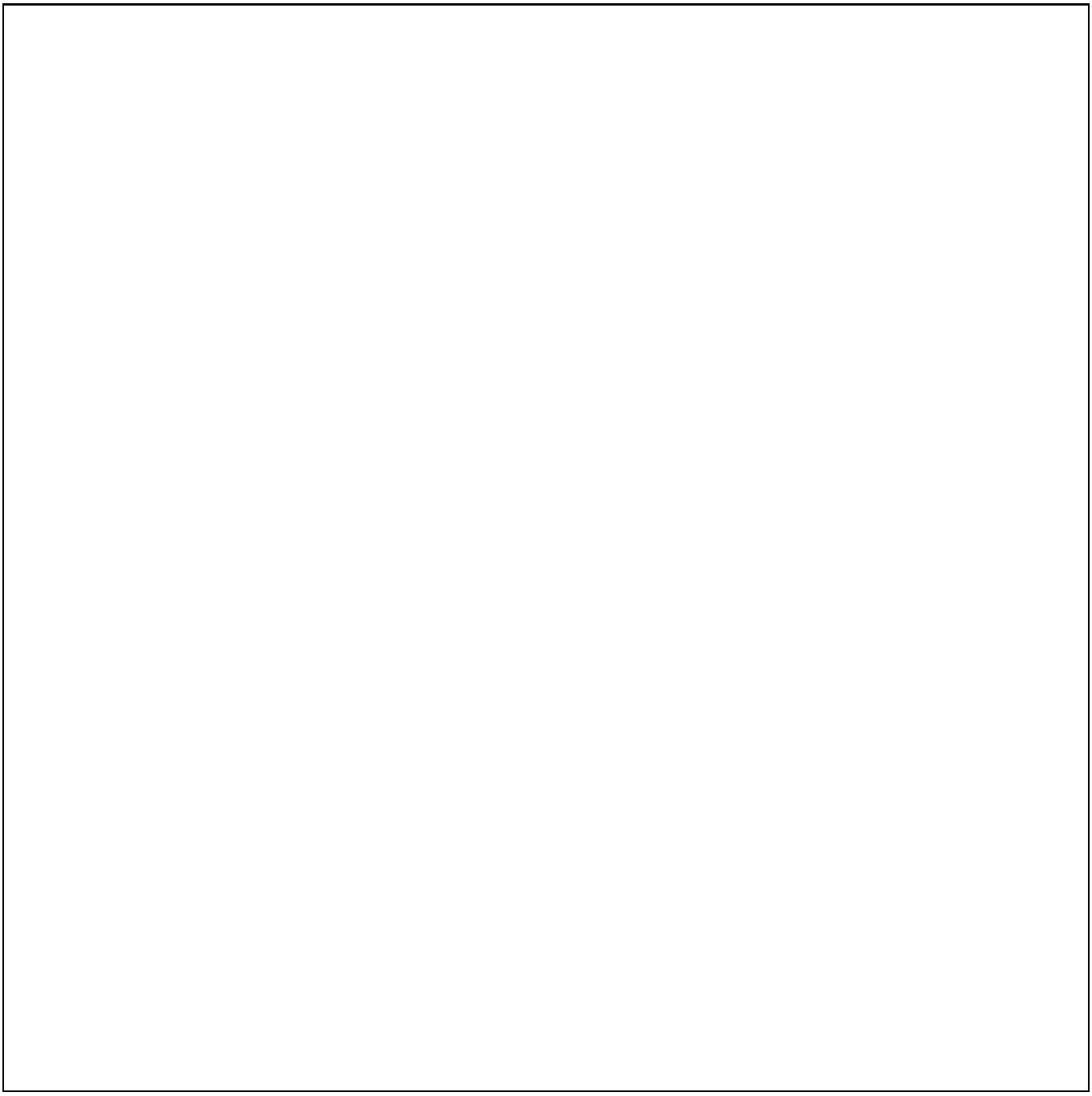

Fig. 1. Field around TON 153. The objects studied spectroscopically are encircled by the slitlet contours

Lyα absorption at the redshift of galaxy # 23 ($z_{\rm g} = 0.6265$) is expected at $\lambda = 1977.29$ Å, whereas the Si II(λ1190) absorption from the $z_{\rm a} = 0.6606$ is detected at $\lambda = 1976.74$ Å). The latter has an asymmetrical shape, and if the blended component at $\lambda = 1977.7$ Å is identified as a Lyα absorption, this leads to a redshift of $z_{\rm a} = 0.6267$, and thus a relative velocity of 50 km s^{-1} from the galaxy. We thus add these three absorption lines to the HST Lyα list, and then find ten galaxies at less than 750 km s^{-1} from a Lyα absorption line.

A Lyα absorption line at $z_{\rm g} = 0.5674$ (slitlet #3) would fall at $\lambda = 1905.4$ Å, where no line is detected at a 3σ level. However, this is only 650 km s^{-1} away from a line identified as Lyβ at $z_{\rm a} = 0.8544$ and quoted as blended in Bahcall et al. (1994). Since we cannot obtain an unambiguous two component fit, we cannot conclude for this case on the absence of Lyα absorption at this galaxy redshift. Similarly, for the galaxy at $z_{\rm g} = 0.3976$ (slitlet #10), there

Table 4. Characteristics of the 3C 351 field

Gal	Δx($''$)	Δy($''$)	θ($''$)	d(kpc)	z_g	z_a	Observations	m_r	M_r
QSO	0.0	0.0	0.0	0.0	0.371			15.28	
1	+264.5	-96.3	281.4	692.2	0.0970		Coinc.[a]	19.8	-19.1
2	+249.7	+29.8	251.4	1549.6	0.3174	0.3172	Lyα	20.7	-21.0
3	+229.7	-90.2	246.7		indef.			21.1	
4	+195.6	-60.2	204.7	498.9	0.0962		Coinc.[a]	16.5	-22.4
5	+155.1	-23.8	156.9	389.3	0.0976		Coinc.[a]	18.5	-20.5
6a	+139.3	-85.0	163.2	934.4	0.2840	0.2845	Lyα	21.0	-20.4
6b	+134.0	-85.9	159.2	296.2	0.0708		Coinc.[b]	18.2	-20.0
7	+105.0	+42.9	113.4	908.8	0.4920		back. gal.	21.5	-21.3
8	+94.1	-15.7	95.4	860.0	0.6217		back. gal.	21.9	-21.6
10	+70.0	+13.3	71.3	347.0	0.2260	0.2229	Lyα	21.3	-19.8
11	+51.2	+17.6	54.1	125.3	0.0910	0.0920	Lyα	18.6	-20.2
12	+31.5	-9.7	32.9	330.6	0.7974		back. gal.	21.5	-22.7
13	+14.2	-30.4	33.6	62.9	0.0713		Coinc.[b]	21.8	-18.0
14	-2.9	+7.0	7.6		indef.			20.7	
15	-26.2	+15.3	30.2		indef.			21.1	
16	-39.5	+46.2	60.6		indef.			20.3	
17	-54.4	+10.2	55.1	394.4	0.4033		back. gal.	21.5	-20.8
18	-73.3	+ 6.8	73.1	310.1	0.1873	0.1880	Lyα	18.2	-22.3
19	-99.4	+127.2	161.4	1440.5	0.6070		back. gal.	20.3	-23.1
20	-115.0	-86.3	143.8	559.7	0.1682	0.1676	Lyα	20.8	-19.4
21	-136.2	+4.3	136.2		indef.			21.5	
22	-148.0	-2.3	148.0	710.6	0.2217	0.2216, 0.2229	metal, Lyα	21.4	-19.5
23	-166.4	-152.7	225.8	1956.2	0.5715		back. gal.	20.7	-22.5
24	-184.4	-134.3	228.1		indef.			19.8	
25	-209.4	-118.1	240.4	1973.8	0.5154		back. gal.	19.8	-23.1
26	-227.5	-101.3	249.0		indef.			21.4	
27	-242.9	-41.2	246.4		indef.			19.8	
28	-261.7	11.0	261.9	1962.7	0.4360		back. gal.	20.4	-22.1

[a] The C II galactic line occurs at less than 750 km s^{-1} from the galaxy redshift (see text).

[b] The geocoronal O I line is at 1302.68 Å whereas the associated Lyα line is expected at 1301.98 Å (see text).

is no absorption at the 3σ level at the expected Lyα wavelength, 1699 Å. However, the very strong Lyβ line of the $z_a = 0.6606$ metal-rich system lies 500 km s^{-1} redward to the latter wavelength, and we also cannot conclude for this case.

For the 8 remaining galaxies with identified redshifts, the wavelength range of the possible, associated Lyα absorption has not yet been observed with the HST.

The completeness of the survey is given in Columns 2 to 4 of Table 2. All the galaxies with associated Lyα-only and metal-rich absorption systems are intrinsically bright ($M_r < -21.1$).

3.2. The field toward 3C 351 (z_{em}=0.371)

There are 14 Lyα-only absorption lines listed in Bahcall et al. (1993), of which two are within 3000 km s^{-1} of the quasar emission redshift. Furthermore, there are two metal-rich systems at $z_a = 0.2216$ and $z_a = 0.3646$. We have obtained spectra for 28 objects in this field, shown in Fig. 2, and get 20 successful identifications, all being galaxies. This field has also been studied by LBTW who identified 11 galaxies, of which six (our slitlets # 5, # 6, # 11, # 12, # 16 and # 18, respectively # 261, # 245, # 187, # 180, # 121 and # 92 in their numbering), are common to our sample. There is a good agreement in the z determination ($\Delta z \leq 0.001$) for galaxies #5, # 6 and # 18, and a small difference for # 11 at $z_g = 0.0910$, for which they measure $z_g = 0.0920$. We did not succeed in measuring a redshift for galaxy # 16, for which LBTW obtain $z_g = 0.2566$. Furthermore, we disagree on the redshift of the galaxy # 12 (# 180 in LBTW). Their spectrum shows two emission lines, around 5000 and 6700 Å, that they identify as [O II]λ3727 and [O III]λ5007 respectively. They do not detect [O III]λ4958, which one would expect given the strong [O III]λ5007

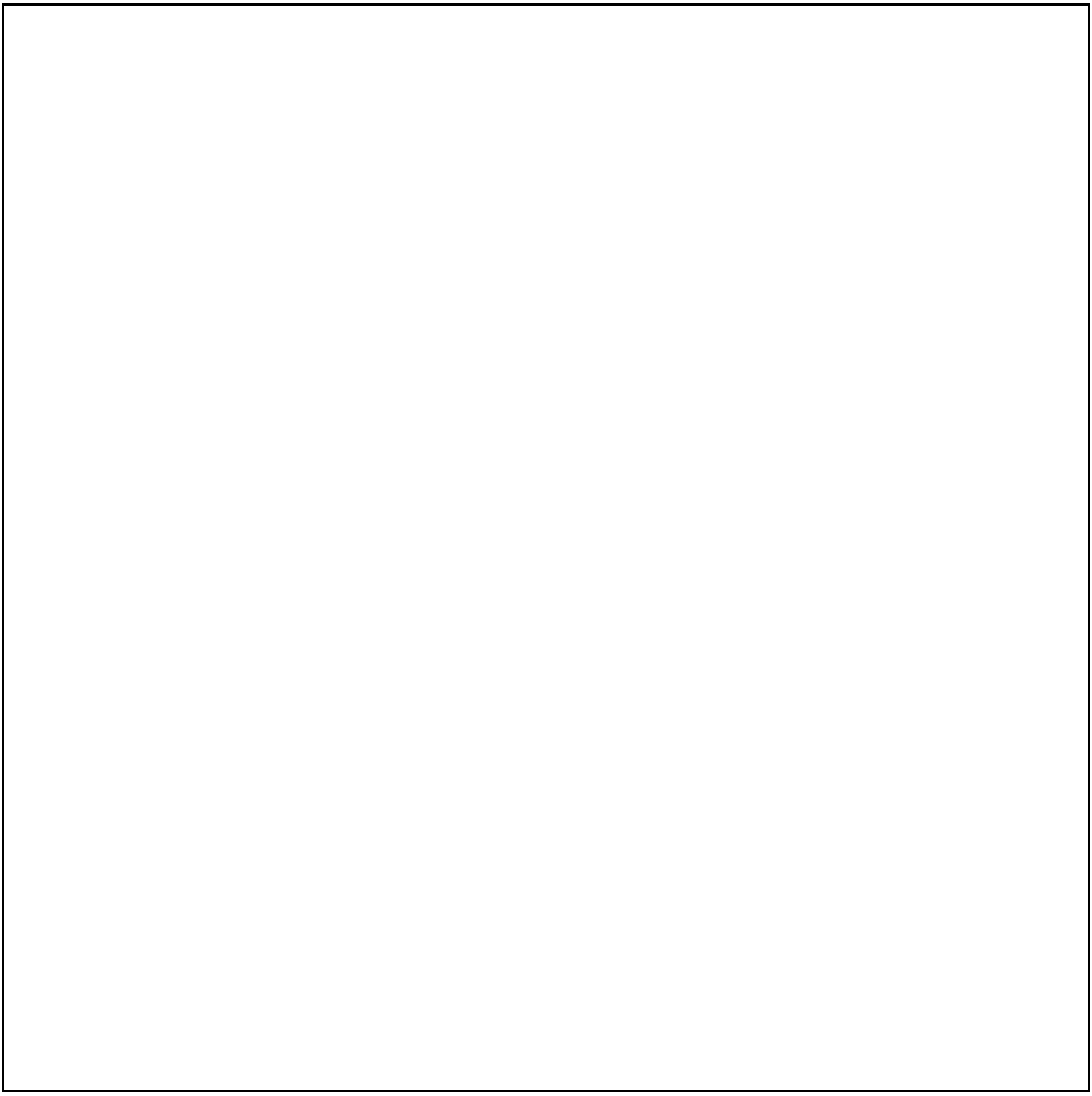

Fig. 2. Same as Fig. 1 for 3C 351

line (see their Fig. 14). We do not detect their [O II] line around 5000 Å, but we identify the line at 6698.89 Å with [O II], since we also detect the Ca II absorption doublet. We then get a redshift of 0.798 for this galaxy.

Among our 20 identified galaxies, seven are at less than 750 km s^{-1} of a Lyα absorption line of the HST complete sample, including # 22 which is at a redshift close that of the $z_{\rm a} = 0.2216$ metal-rich system, but with a very large impact parameter ($l = 710 h_{50}^{-1}$ kpc). Three other have nearly the same redshift $z_{\rm g} \simeq 0.097$, and one then expects an associated Lyα line at $\lambda = 1333.59$ Å. No line is present at this wavelength in the HST sample, but the C II(λ1134) Galactic line is detected only 600 km s^{-1} away. There is an indication of an asymmetrical shape for this line, but only high resolution spectroscopy could confirm this. The same problem occurs for the two galaxies # 6b and # 13 at $z_{\rm g} \simeq 0.071$, for which an associated Lyα line would be at $\lambda = 1301.98$ Å, close to the very strong geocoronal O I

Table 5. Characteristics of the H 1821+6419 field

Gal	Δx($''$)	Δy($''$)	θ($''$)	d(kpc)	z_g	z_a	Observations	m_r	M_r
QSO	0.0	0.0	0.0	0.0	0.297			14.24	
1	+273.4	+85.9	286.6	692.2	0.0000		star	20.7	
2	+255.2	+47.5	259.6	1534.3	0.2977		QSO cluster	18.6	-23.0
3	+233.3	+72.0	244.2	1652.3	0.3672		back. gal.	19.9	-22.2
4	+215.4	+71.7	227.1	1925.5	0.5482		back. gal.	21.7	-21.4
5	+192.0	+83.6	209.4	1243.5	0.2998		QSO cluster	20.1	-21.5
6	+174.4	+8.8	174.6	1016.1	0.2909		QSO cluster	18.9	-22.6
7	+148.7	+24.9	150.8	889.0	0.2966		QSO cluster	20.1	-21.5
8	+132.3	+50.9	141.8	556.8	0.1703	0.1704	Lyα	16.9	-23.3
9	+114.1	+90.3	145.5	843.5	0.2890		QSO cluster	18.8	-22.7
11	+81.9	+42.5	92.2	544.0	0.2970		QSO cluster	18.4	-23.2
12	+61.6	-27.1	67.3	392.6	0.2920		QSO cluster	19.7	-21.8
13	+38.9	+16.1	42.1	246.6	0.2938		QSO cluster	19.5	-22.0
14	+14.2	-31.3	34.4	201.1	0.293		QSO cluster	18.8	-22.7
15	-4.9	+8.1	9.5	56.6	0.3013		QSO cluster	18.8	-22.8
16	-25.1	-7.0	26.1	153.3	0.295	0.2972	metal	20.5	-21.1
17	-47.9	+16.5	50.6	289.9	0.2844		QSO cluster	20.7	-20.7
18	-61.0	-45.8	76.3	455.1	0.3018		QSO cluster	19.8	-21.8
19	-87.1	-7.0	87.4	509.5	0.2917		QSO cluster	18.9	-22.6
20	-106.6	-21.5	108.8	641.8	0.2969		QSO cluster	20.7	-20.9
21	-131.4	+3.8	131.5	781.2	0.3000		QSO cluster	19.5	-22.1
22	-149.1	+70.7	165.1	672.6	0.1785	0.1806	Lyα	20.3	-21.0
23	-184.5	+125.9	223.3	952.4	0.1894		$w_r \leq 0.15$ Å[a]	19.3	-22.2
24	-202.0	+3.5	202.0	1187.3	0.2953		QSO cluster	19.8	-21.7
25	-225.6	-61.3	233.8	1392.0	0.301		QSO cluster	19.4	-22.2
26	-244.2	+15.6	244.7	1456.9	0.3010		QSO cluster	20.0	-21.6

[a] This is the 4.5σ equivalent width limit for an associated Lyα absorption.

emission line at $\lambda = 1302.68$ Å. Thus, no conclusion can be reached in this case either. The eight remaining objects are background galaxies. We do not observe any unambiguous case of a galaxy which does not give rise to a Lyα absorption line. Information on the galaxy counts in different magnitude bins is given in Columns 5 to 7 of Table 2. The completeness is calculated including the redshifts obtained by LBTW, which correspond to the numbers in bracket in Column 6. When a galaxy is common to the two samples, we adopt our own redshift determination.

In this field, the galaxies with a redshift close to that of a Lyα system are less luminous in average than in the field of TON 153 ($M_r < -19.4$).

3.3. The field toward H 1821+6419 (z_{em}=0.297)

The HST complete sample of absorption lines contains 12 Lyα-only absorption systems and one high-ionization metal-rich system with C IV and Si IV absorption lines at the quasar redshift. In this field (see Fig. 3) we measured the redshifts of the 25 objects which were in the slitlets, all being fairly bright ($m_r \leq 21.0$). The sample contains one star and 24 galaxies, of which two are background galaxies, two are at less than 650 km s^{-1} of a Lyα absorption line, and 19 other galaxies are within 4000 km s^{-1} of the quasar redshift. They confirm the presence of a cluster at $z_a \simeq z_e = 0.2972$, already inferred by Schneider et al. (1992). From these 19 galaxies, we get a value of 1100 km s^{-1} for the velocity dispersion.

The remaining galaxy has a redshift of $z_g = 0.1894$, and there is no Lyα absorption line detected in the quasar spectrum at this redshift. The 4.5σ rest equivalent width limit is 0.15 Å, and the nearest Lyα system is 2200 km s^{-1} away.

Schneider et al. (1992) have also studied this field and measured the redshifts of eight galaxies, none of them being common to our sample. They found 6 galaxies at $z_g \simeq z_e$, one background galaxy and one at a redshift close to that

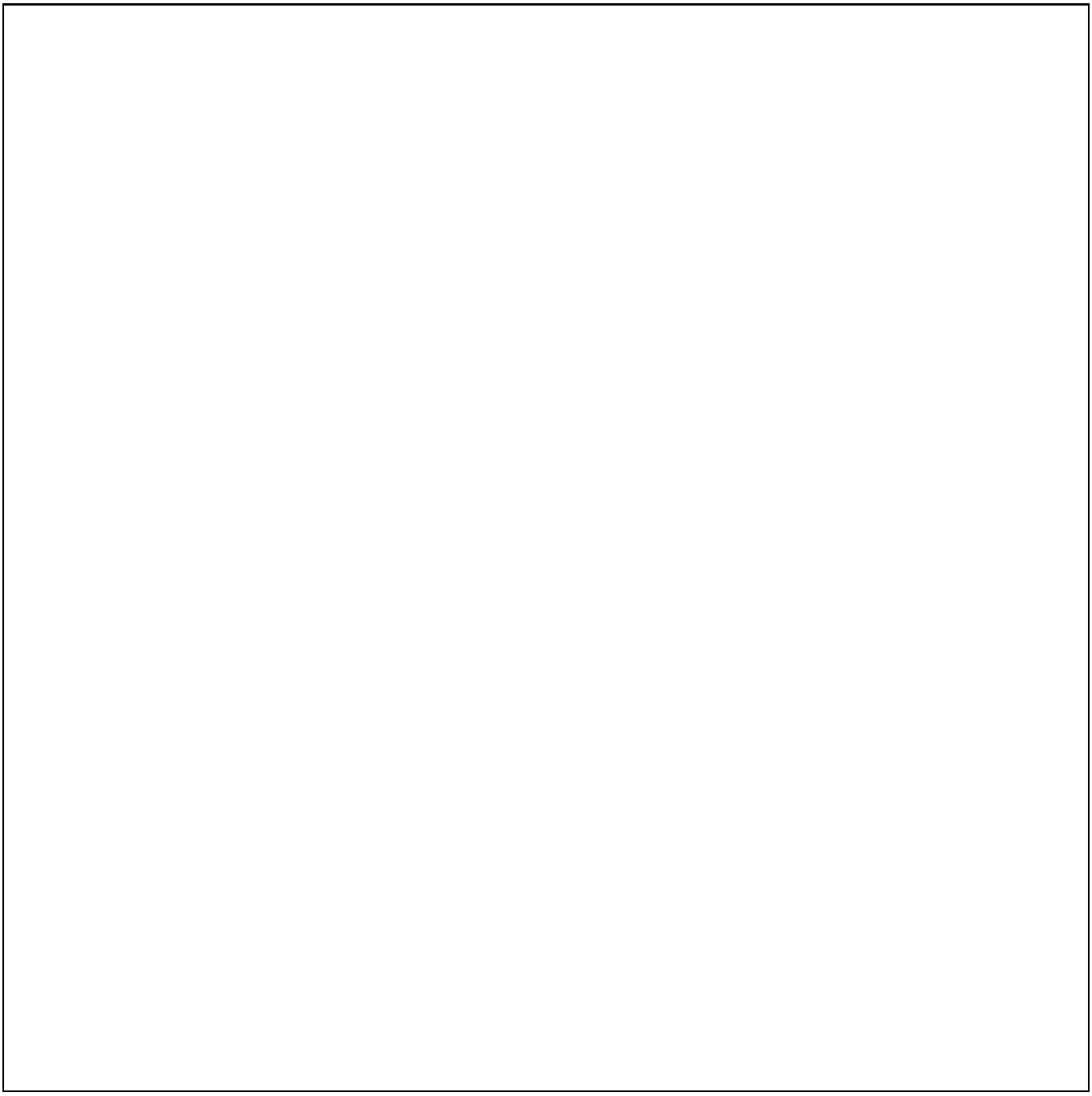

Fig. 3. Same as Fig. 1 for H 1821+6419

of a Lyα system at $z_{\rm a} = 0.2265$. The completeness of the redshift survey (Columns 8 to 10 of Table 2) is calculated including their redshift measurements, which are given in brackets in Column 9.

The nebulosity North-West to the quasar is the planetary nebula Kohoutec 1-16.

3.4. Overall results

We have obtained the spectra of 81 objects for the three combined fields. We identified two stars and could determine 66 galaxy redshifts, thus a success rate of 81%. The very small number of stars in our sample is a consequence of having selected resolved objects. Since the selection was made using high resolution imaging data (0.6″ FWHM) of

the central parts of the fields, we were able to include compact galaxies in our sample. Among the 66 galaxies with measured redshift, 19 (16) are at less than 750 (500) km s^{-1} of a Lyα absorption system.

Of the remaining galaxies, only one clearly does not have an associated Lyα absorption, whereas seven galaxies have an expected, associated Lyα absorption possibly blended with either a geocoronal line, a Galactic line or a metal-line from another system. Higher resolution data are needed to draw any conclusion on these seven cases. The relative velocity between four galaxies and a metal-rich system is less than 600 km s^{-1}; one of these galaxies belong to the above sample of Lyα-only-galaxy associations. There are 18 galaxies from the cluster associated with the quasar H 1821+6419 and ten background galaxies. Finally, there are eight galaxies, all in the field of TON 153, for which there is no available data in the wavelength range of the expected, associated Lyα absorption.

4. Properties of Lyα absorbers

4.1. The samples

4.1.1. The Lyα sample

The rest-frame equivalent width limit for the HST spectra of 3C 273 are much lower than those obtained for the other quasars discussed here or by LBTW. We thus select Lyα systems with $w_{\rm r}\,({\rm Ly}\alpha) \geq 0.10$ Å, limit consistent with the weakest systems detected in the quasar spectra of our sample.

The Lyα absorption lines detected only in low-resolution FOS spectra are excluded from the combined sample. This resolution, $R = 180$, is seven times lower than that obtained with the higher resolution mode, and very strong lines could be blends of several lines or damped Lyα lines from a metal-rich system. Indeed, lines as strong as $w_{\rm r} \geq 1.5$ Å detected in the $R = 1300$ resolution mode are all associated with metal-rich systems and are not present in the homogeneous sample of 109 Lyα-only systems build from the 17 Key Project quasar spectra (Bahcall et al. 1994). Since metal-rich systems are known to be physically associated with galaxies, they are not included in the Lyα sample, as this could introduce a bias in the statistical analyses of the Lyα absorber population.

4.1.2. The galaxy and the Lyα absorber-galaxy association samples

Three other teams obtained galaxy redshift samples for HST quasar fields. LBTW have studied 8 fields and their relative velocity criterion for assigning absorption systems to galaxies is $|\Delta v| \leq 1000$ km s^{-1}. Their sample remains unmodified if our criterion ($|\Delta v| \leq 750$ km s^{-1}) is applied instead, since it does not contain any association with an absolute relative velocity in the range 750-1000 km s^{-1}. Morris et al. (1993) have obtained complete, magnitude limited samples of over 200 galaxies in the field of 3C 273. These samples were defined to carry out a correlation analysis and are complete to faint magnitude limit out to a large impact parameter of $16h_{50}^{-1}$ Mpc. For their sample of 17 Lyα absorber-galaxy associations, the largest velocity separation is 710 km s^{-1}, but only 120 km s^{-1} for impact parameters smaller than $2.5h_{50}^{-1}$ Mpc. The small sample studied by Schneider et al. (1992) contains only one galaxy at $z_{\rm g} \simeq z_{\rm a}\,({\rm Ly}\alpha) \neq z_{\rm e}$ and the relative velocity is 340 km s^{-1}. Consequently our relative velocity selection criterion does not exclude any galaxy from the samples obtained by the above mentioned teams. For the cases in common with LBTW, we use our own redshift estimates.

The criteria for assigning a galaxy to a Lyα absorption line are the smallest relative velocity and impact parameter. Even though the galaxy sample is far from being complete, the additional second criterion is needed in two cases: the close pair at $z_{\rm g} = 0.5397 \simeq z_{\rm a} = 0.5436$ in the field of TON 153 and the two galaxies at $z_{\rm g} \simeq z_{\rm a} = 0.2229$ in the field of 3C 351. This leads to a total sample of 32 Lyα absorber-galaxy associations, of which two are in common with the sample of LBTW, and to a sample of 11 galaxies without associated Lyα absorption. The combined sample is given in Table 6.

4.2. Significance of the Lyα absorber-galaxy associations

In discussing the relation between the galaxies found in the field of each quasar and Lyα lines, it is important to assess the significance level of the "associations" defined above. In other words, can we rule out that they are just due to chance? First of all, one has to decide in which manner the distance between the absorber and the "associated" galaxy is to be estimated. As discussed by Morris et al. (1993), one should compute the 3-dimensional distance which involves both the separation in depth (related to the redshift difference) and the impact parameter. However, it is straightforward to verify (for instance using the formulas given by Tytler et al. (1993) for $q_0 = 0.5$) that the contribution of the "transverse" term can be neglected. Indeed, for a Δz value corresponding to $\Delta v = 100$ km s^{-1} and an angular

Table 6. The combined sample of identified Lyα systems

Quasar	Author	z_a	w_{rest}	z_g	d(kpc)	M_r	Δv
TON 153 (1317+2743)	This work.						
		0.5349	0.29	0.5324	1624.0	-21.3	490
		0.5436	0.10	0.5397	563.5	-22.3	750
		0.6267	0.11	0.6265	1421.1	-22.8	40
		0.6692	0.60	0.668	1242.4	-23.2	220
		0.6716	0.39	0.6715	77.5	-22.0	20
		0.6736	0.78	0.6717	415.3	-21.3	340
		0.6947	0.34	0.6952	1669.7	-22.0	-90
		0.6958	0.40	0.6974	996.9	-21.4	-280
		0.7667	0.12	0.7663	2375.7	-21.3	70
3C 351 (1704+6048)	This work.						
		0.0920	0.82	0.0910	125.3	-20.2	280
		0.1676	0.23	0.1682	559.7	-19.4	-150
		0.1880	0.36	0.1873	310.1	-22.3	180
		0.2229	0.34	0.2260	347.0	-19.8	-750
		0.2845	0.62	0.2840	934.4	-20.4	120
		0.3172	0.64	0.3174	1549.6	-21.0	-50
3C 351 (1704+6048)	Lanzetta et al.[a]						
		0.0920	0.82	0.0922	125.3	-20.2	280
		0.1611	0.29	0.1621	718.8	-22.9	-260
		0.1880	0.36	0.1875	310.1	-22.3	130
		0.3621	0.49	0.3621	189.2	-21.5	0
		0.3716	0.26	0.3709	301.6	-23.7	150
			< 0.16	0.0860	325.3	-21.0	
H 1821+6419	This work						
		0.1704	0.64	0.1703	556.8	-23.3	30
		0.1806	0.30	0.1785	672.6	-21.0	530
			< 0.15	0.1894	952.4	-22.2	
H 1821+6419	Schneider et al.						
		0.2251	0.75	0.2265	158.2	-22.1	-340
1354+1933	Lanzetta et al.[a]						
		0.4306	1.03	0.4302	210.5	-20.5	80
			< 0.25	0.3509	543.9	-20.6	
			< 0.15	0.4406	187.0	-21.3	
			< 0.15	0.5293	415.6	-21.4	
TON 28 (1001+2910)	Lanzetta et al.[a]						
		0.2132	0.57	0.2127	341.8	-22.4	120
			< 0.08	0.1343	247.3	-21.2	
US 1867 (0850+4400)	Lanzetta et al.[a]						
		0.4435	0.51	0.4428	77.9	-21.8	150
			< 0.24	0.4259	380.8	-21.4	
			< 0.08	0.5065	210.0	-21.9	
			< 0.09	0.5200	375.5	-23.0	
3C 95 (0349−1438)	Lanzetta et al.[a]						
			< 0.17	0.4223	584.9	-22.0	
			< 0.11	0.5526	602.8	-22.2	
3C 273 (1226+0219)	Morris et al.[b]						
		0.0034	0.37	0.00333	1376.0	-18.6	20
		0.0053	0.41	0.00524	368.0	-17.3	20
		0.0073	0.24	0.00745	944.0	-16.2	-50
		0.0294	0.12	0.02938	560.0	-18.1	20
		0.0490	0.14	0.04957	2592.0	-18.8	-160
		0.0666	0.30	0.06892	7600.0	-20.0	-650
		0.1201	0.11	0.12067	3056.0	-20.2	-180
		0.1466	0.29	0.14668	1600.0	-21.3	-20

[a] The sample of LBTW has been reduced to the high resolution data, excluding the G160L data.
[b] The sample of Morris et al. (1993) is restricted to w_r (Lyα) ≥ 0.10 Å.

separation $\Delta\theta = 3'$ at $z = 0.5$, the latter barely equals the separation in depth. Then, for simplicity we consider the comoving distance in depth only, which for small redshift differences reduces to

$$d = \left(\frac{c}{H_0}\right) \frac{|\Delta z|}{(1+z)}. \quad (1)$$

Since our galaxy sample is not complete, we first consider the detected galaxies, and for each of them search for the nearest Lyα line. In order to get homogeneous results for our three quasar fields, we restrict our search to Lyα lines with a rest-frame equivalent width $w_r \geq 0.24$ Å, and thus consider only the systems included in the complete samples of the HST absorption line survey (Bahcall et al. 1993, 1994) (the deblended lines in the spectrum of TON 153 quoted in Table 3 are not considered). Given the differences in S/N ratios and redshift ranges, such lines can be detected over the redshift intervals 0.39-1.00, 0.05-0.357 and 0.0-0.285 in TON 153, 3C 351 and H 1821+6419 respectively. The same redshift intervals are used for the galaxy sample. As a measure of the overall match between the sets of redshifts of Lyα absorbers and galaxies, Morris et al. (1993) consider the average of the nearest distance over all galaxies. However, this quantity gives much weight to a single galaxy far from any Lyα line even if several close associations are present, i.e. few anti-coincidences may hide several significant coincidences. We thus prefer instead to count the number of "associations" found for the following relative velocity criteria: $|\Delta v| < 750$ km s^{-1}, the value adopted above, $|\Delta v| < 400$ km s^{-1}, which is roughly the cutoff in the relative velocity distribution (see Sect. 4.1) and $|\Delta v| < 250$ km s^{-1}, which is about the average galactic inner velocity dispersion.

Table 7. Significance of the Lyα absorber-galaxy associations

Quasar field	z interval	N_{gal}	N_{syst}	$N^a_{1,obs}$	$N^a_{2,obs}$	$N^a_{3,obs}$	P^b_1	P^b_2	P^b_3
TON 153	0.39 - 1.000	13	26	4	5	6	0.059	0.062	0.18
3C 351	0.05 - 0.357	7	12	4	6	6	0.001	$5\ 10^{-4}$	$5\ 10^{-4}$
H 1821+6419	0.0 - 0.285	3	11	1	1	2	0.22	0.33	0.11
combined		23	49	9	12	14	$5\ 10^{-5}$	$5\ 10^{-5}$	$5\ 10^{-5}$

[a] $N_{1,obs}$, $N_{2,obs}$, $N_{3,obs}$ are the observed numbers of Lyα absorber-galaxy pairs with $|\Delta v| \leq 250$, 400, 750 km s^{-1}respectively
[b] P_1, P_2, P_3 are the probabilities to have by chance at least $N_{1,obs}$, $N_{2,obs}$ or $N_{3,obs}$ Lyα absorber-galaxy pairs with $|\Delta v| < 250$, 400, 750 km s^{-1} respectively

To judge whether the observed number of redshift agreements is significant or not, we perform Monte Carlo simulations. The same redshift intervals are used together with the same galaxy redshifts for each quasar field. Next, Lyα redshifts are selected at random in the appropriate interval and with a mean distribution of the form (Bahcall et al. 1994):

$$\frac{\mathrm{d}N}{\mathrm{d}z} \propto (1+z)^{0.5}, \quad (2)$$

with the same number of lines than the observed one. Each simulation is then analyzed in the same way as the original data (search for the nearest line to each galaxy) and we thus derive the probability to get by chance a number of associations which is equal to the observed one or greater. This is done first for the three quasar fields separately and then globally. For the latter case, a simulation consists in joining three individual ones for each of the three quasar fields and in considering the total number of associations. Results are given in Table 7. The associations are not statistically significant for individual fields, except for 3C 351, but for the combined sample the existence of redshift agreements is found to be highly significant.

4.3. Search for correlations

4.3.1. Impact parameter and rest-frame equivalent width

LBTW have found a statistically significant anti-correlation between the Lyα rest-frame equivalent width and the galaxy impact parameter (see their Fig. 24). On the basis of their results, they conclude that most luminous galaxies are surrounded by extended gaseous envelopes of radius $R \simeq 345 h_{50}^{-1}$ kpc and of roughly unit coverage factor. Their

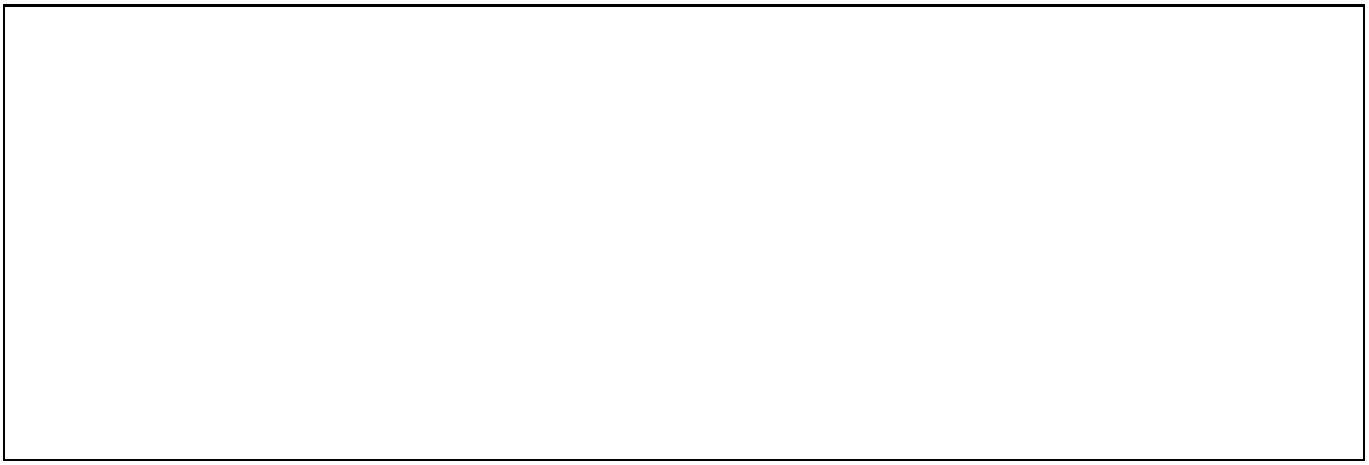

Fig. 4. Impact parameter versus Lyα rest-frame equivalent width. Crosses: This work, Hexagons: Lanzetta et al. (1995), Stars: Morris et al. (1993), Diamonds: Schneider et al. (1992)

sample includes 11 Lyα absorber-galaxy associations of which two are metal-rich absorbers and one is a very strong Lyα absorber detected only in low spectral resolution data.

If all the Lyα absorbers were a single population, analyses of subsamples selected either by the strength of Lyα absorption or the metal content should lead to similar correlations. Since the impact parameters of strong metal-rich absorbers are known to be smaller than those for Lyα clouds, it is appropriate to search independently for correlations among the "Lyα-only" population. To investigate the $w_{\rm r}$ (Lyα) -D relation, we have first considered our homogeneous sample which excludes metal-rich systems. We do not confirm the anti-correlation previously found (see Fig. 4). The results of the generalized Spearman and Kendall rank-correlation tests are given in Table 8. The parameters $\alpha_{\rm s}$ and $\alpha_{\rm k}$ are the probabilities that the values of the coefficients obtained for our distribution, $r_{\rm s}$ and $r_{\rm k}$, are reached if the data are uncorrelated. As LBTW, we have included the upper limits. We have used the method presented in Isobe et al. (1986) and implemented in the software package ASURV Rev1.1 (La Valley et al. 1992). If the sample is restricted to $w_{\rm r} \geq 0.24$ Å, criterion limit selected by Bahcall et al. (1993, 1994) for complete Lyα samples, there is a weak anti-correlation between D and $w_{\rm r}$ (Lyα) at the 90% confidence level. Adding to our whole combined sample the previously excluded three strong Lyα systems of the Lanzetta et al.' survey strongly modifies the results of the rank statistics, the anti-correlation being then present at the 97% confidence level.

Stocke et al. (1995) have recently found eight new low-redshift Lyα-only systems, of which seven are absorber-galaxy associations. As in the case of Morris et al.' survey, all the galaxies are at large impact parameters ($\geq 675 h_{50}^{-1}$ kpc) and they conclude that none of the absorbers is close enough to an individual galaxy to be unambiguously associated with it. They have combined their results with previously published data, including only absorber-galaxy associations. Analysis of their sample shows an anti-correlation between D and $w_{\rm r}$ (Lyα), which is not as tight when only low equivalent widths ($w_{\rm r} < 0.30$ Å) are considered. This trend is similar to that found for our sample when dividing it into strong and weak lines.

It should be noted that excluding all the censored cases with only $w_{\rm r}$ (Lyα) upper limits could lead to results which strongly differ from those obtained with complete samples. Ordinary rank statistics applied to the 32 absorber-galaxy associations of our combined sample reveals a strong anti-correlation between D and $w_{\rm r}$ (Lyα) at the 99.5% confidence level, which however is not as significant (95% confidence level) at high equivalent widths, $w_{\rm r} \geq 0.24$ Å. Adding to our 32 associations, the three strong Lyα absorbers of Lanzetta et al.' survey, leads to a very strong anti-correlation (99.98% confidence level).

The differences in the results found with ordinary and generalized rank statistics call for caution in drawing conclusions. There appears to be a weak anti-correlation between D and $w_{\rm r}$ (Lyα), which is of higher significance when either metal-rich Lyα systems or stronger Lyα absorbers are considered for complete samples with the $w_{\rm r}$ (Lyα) upper limits included. These results do not support the single population hypothesis.

The Lyα absorber-galaxy associations with smaller impact parameters could trace extended galactic halos. Indeed, all the four galaxies of the combined sample with impact parameters $D \leq 175 h_{50}^{-1}$ kpc have associated Lyα-only absorption, whereas this is also the case for only about half of them for $175 < D \leq 1000\ h_{50}^{-1}$kpc. These results are not significantly modified if the combined sample is restricted to galaxies brighter than an absolute magnitude limit, $M_{\rm r} = -19$, which is the magnitude limit of our survey at $z \simeq 0.3$. This selection criterion excludes the galaxies at

$z < 0.06$ of the survey of Morris et al. (1993). It should be noted that all the six galaxies at $1 < D < 2\ h_{50}^{-1}$Mpc and brighter than $M_r = -19$ have an associated Lyα absorption. Consequently, we detect a break in the number of Lyα absorber-galaxy associations relative to the total number of galaxies at $D \simeq 200 h_{50}^{-1}$ kpc, with a flattening at larger values of D (see also Sect. 5). This critical value of D, which should give the average size of galactic halos, is nearly twice as small as that found by LBTW. This difference mainly arises from having included in our sample a large number of absorber-galaxy associations detected either in our survey or that of Morris et al. (1993).

Table 8. Correlations

Variables	r_s	α_s	r_k	α_k
D , w_r	-0.141	0.359	1.034	0.301
D , w_r [a]	-0.336	0.087	1.650	0.099
M_r , $\log(D)$	-0.243	0.115	1.527	0.127
w_r , $\lvert\Delta v\rvert$	-0.034	0.851	0.098	0.922
D , $\lvert\Delta v\rvert$	0.124	0.489	0.716	0.474

[a] Sample restricted to w_r (Lyα) ≥ 0.24 Å

4.3.2. Relative velocity distribution

Although the adopted relative velocity criterion for assigning a galaxy to a Lyα absorption system is $|\Delta v| \leq 750$ km s^{-1}, the relative velocity distribution of Lyα absorber-galaxy associations, as shown on Fig. 5, is narrow, roughly centred on $\Delta v = 0$ km s^{-1} and symmetrical, whereas the expected histogram for a random distribution is flat. The half-width, half maximum of this distribution is HWHM $\simeq 120$ km s^{-1}and 77% of the 32 Lyα absorber-galaxy associations have $|\Delta v| \leq 300$ km s^{-1}.

This narrow velocity distribution is compatible with spiral galaxy rotation velocities. Its mean is smaller than the median velocity dispersion of ~ 500 km s^{-1} which characterizes the thickness of the sheets of large-scale structures (Ramella et al. 1989, 1992). This velocity dispersion has been derived by averaging within cells of sizes $\sim 10 h_{50}^{-1}$ Mpc, i.e. over one order of magnitude larger than the typical projected distances between Lyα absorber-galaxy associations. The local thickness of large-scale structures can be derived from the CFA redshift survey of close galaxy-pairs and it is about a factor of three smaller than the above median velocity dispersion (M. Geller, private communication). The small HWHM of the relative velocity distribution of the Lyα absorber-galaxy associations is thus also consistent with the assumption that most Lyα absorbers trace large-scale structures rather than individual objects, at least for impact parameters $D > 200$ to $300\ h_{50}^{-1}$ kpc.

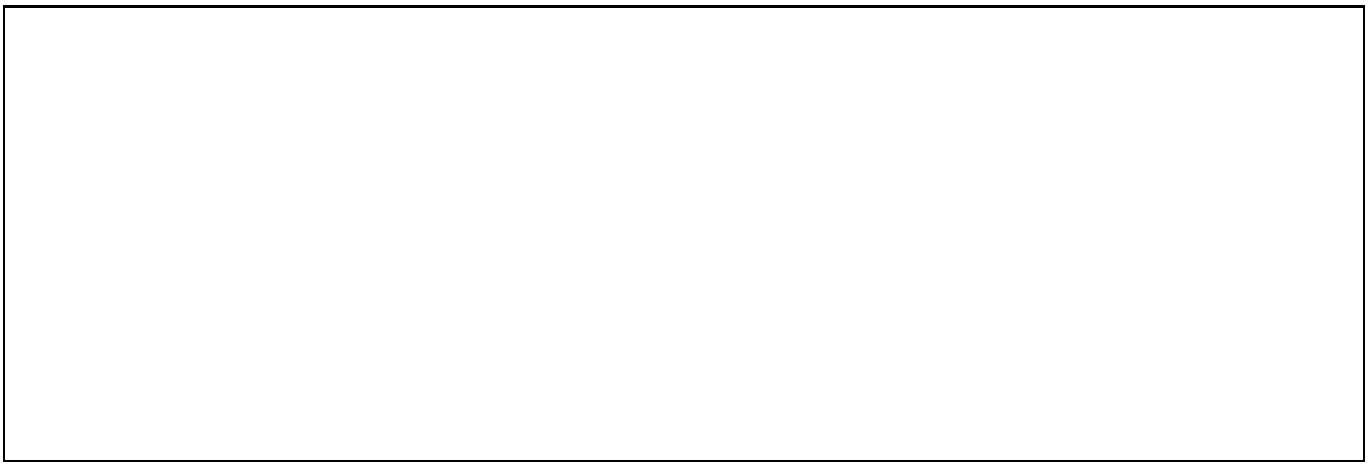

Fig. 5. Relative velocity distribution

4.3.3. Impact parameter and luminosity

For the metal-rich absorption systems, the scaling law between the stellar luminosity and the galactic halo radius follows a power law, $D \propto L^{\alpha}$, with $\alpha = 0.2$ to 0.3 (Bergeron & Boissé 1991; Steidel 1993). This correlation is not as strong as that found for galactic stellar component for which the Schwarzschild scaling law implies $\alpha \simeq 0.42$. We investigate the existence of such a correlation for the Lyα absorber-galaxy associations. Results are given in Fig. 6 and Table 7, from which it is clear that the impact parameter and the galaxy luminosity are uncorrelated.

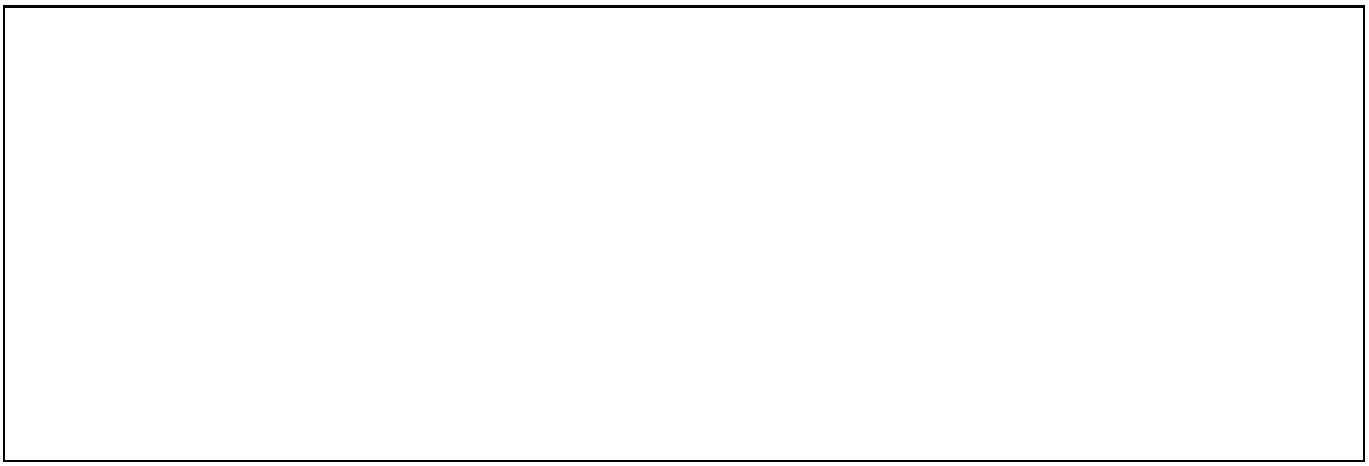

Fig. 6. Luminosity of the galaxy versus impact parameter, and same notations as in Fig. 4

There is an overlap in impact parameters between the metal-rich and Lyα-only absorbers. As the Lyα absorbers of smallest impact parameters have larger rest-frame Lyα equivalent widths, the continuity in sizes and H I column densities between the two populations strengthens the assumption that at least the strongest Lyα absorbers trace the outermost parts of galactic halos. The lack of correlation between the impact parameter and the luminosity, even for $D < 300 h_{50}^{-1}$ kpc, may suggest that the size of the Lyα galactic halos is linked to the total mass, which at large galactic radii is dominated by the dark matter, whereas at smaller radii both the baryonic (mainly in the form of stars) and dark matter components contribute to the total mass.

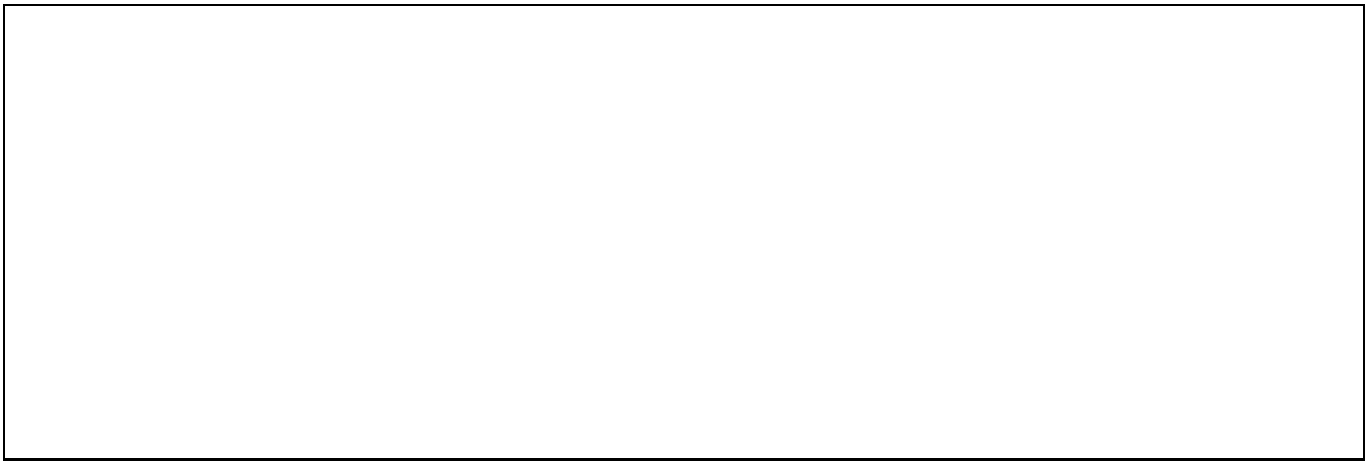

Fig. 7. Impact parameter versus Lyα absorber-galaxy relative velocity, and same notations as in Fig. 4

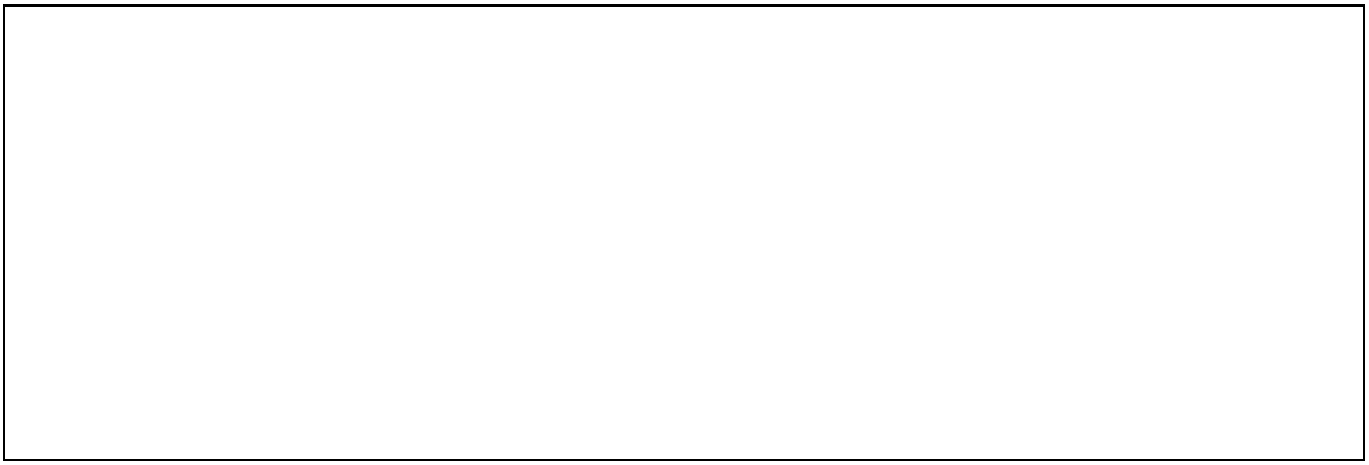

Fig. 8. Lyα rest-frame equivalent width versus Lyα absorber-galaxy relative velocity, and same notations as in Fig. 4

4.3.4. Search for other correlations

There is no correlation between the Lyα absorber-galaxy relative velocity and the impact parameter or the Lyα rest-frame equivalent width (see Table 7 and Figs. 7 and 8). The former suggests a lack of organized motions on scales 0.3-1.5 h_{50}^{-1} Mpc, consistent with the assumption that a large fraction of the Lyα absorber-galaxy associations trace coherent large-scale structures rather than individual galaxies.

4.4. Clustering of Lyα systems and galaxies

The complete galaxy survey of Morris et al. (1993) towards 3C 273 has allowed a study of the two-point correlation function of Lyα absorber-galaxy pairs. These authors have shown that, although the Lyα absorbers are not distributed at random with respect to galaxies, they are clustered around galaxies less strongly than the galaxies themselves are, in particular over length scales of 1.6 to $16h_{50}^{-1}$ Mpc.

The Lyα absorption systems show clustering on velocity scales of 1000 to 3000 km s^{-1} (Bahcall et al. 1994), thus larger than observed for galaxies within groups and sheets of large-scale structures (Ramella et al. 1989) and closer to velocity spreads found for cluster or superclusters of galaxies. Furthermore, about half of the extensive metal-rich absorption systems are accompanied by such clumps of neighboring Lyα absorption lines. Our galaxy sample can be used to investigate the occurrence of galaxy clumps, on similar velocity scales, associated with one or more Lyα absorption lines. To conduct this study, we select Lyα absorption lines (including metal-rich systems) satisfying the same criterion limit as used by Bahcall et al. (1993, 1994), $w_{\rm r} \geq 0.24$ Å.

The clumps of Lyα lines and associated galaxies, with impact parameters up to $1.6h_{50}^{-1}$ Mpc, are listed in Table 9. The largest grouping of Lyα lines is found towards the quasar TON 153. There are five Lyα-only lines at $z_{\rm a} \simeq 0.67 \ll z_{\rm e}$, clustered within 1400 km s^{-1} ; including a neighboring metal-rich system leads to a total velocity span of about 3000 km s^{-1}. At least four of these six absorption systems have an associated galaxy. Towards the same quasar, there is also a pair of Lyα absorbers at $z_{\rm a} \simeq 0.54$ with three associated galaxies (of which two form an interacting pair) spanning about 1500 km s^{-1}. In addition the sample includes one triplet and six pairs of Lyα lines spanning from 320 to 2950 km s^{-1}. The triplet and one of the pairs include one metal-rich system. For about half of these Lyα absorbers, there is a detected, associated galaxy.

The sample also contains groups of galaxies associated with a single Lyα absorption line. There is a rich cluster of galaxies detected towards the radio-quiet quasar H 1821+6419, with 25 galaxies at $z_{\rm g} \simeq z_{\rm a} \simeq z_{\rm e} = 0.297$ (including the galaxies observed by Schneider et al. 1992), spanning about 4000 km s^{-1} and with a velocity dispersion of 1100 km s^{-1}. The second largest grouping of galaxies is detected towards the quasar 3C 351, with four galaxies at $\langle z_{\rm g} \rangle = 0.0973$ and spanning only 380 km s^{-1}, indicative of a physical group. Unfortunately, the associated Lyα absorption is expected at $\lambda_{\rm obs} = 1334.0$ Å and would be heavily blended with the strong Galactic C II($\lambda_{\rm obs} = 1334.5$ Å) absorption. The pair of galaxies at $z_{\rm g} = 0.0710$ is also another inconclusive case : the impact parameters for both galaxies are $D < 350h_{50}^{-1}$ kpc and their relative velocity is $\Delta v = 140$ km s^{-1}, but the associated Lyα absorption line would be blended with the strong O I Geocoronal emission line. The interacting pair of galaxies at $z_{\rm g} = 0.5398$ is associated to a single Lyα absorber and it should be embedded in a supergiant halo of radii of order $600h_{50}^{-1}$ kpc. This could also be the case for

Table 9. Clustering of Lyα systems and galaxies

N_a	z_a	$\lvert\Delta v_{a-a}\rvert$ km s^{-1}	N_g	z_g	d kpc	Size kpc × kpc	Mag	$\lvert\Delta v_{g-g}\rvert$ km s^{-1}	Nature
						TON 153			
2	0.5349	2050	3	0.5324	1624.0	2300×100	−21.3	1450	Lyα
	0.5454			0.5397	563.5		−22.3		
				0.5398	578.4		−22.0		
6	0.6606	3000	4	0.6639	1471.1	1500×300	−22.4	1400	metal
	0.6692			0.668	1242.4		−23.2		and Lyα
	0.6716			0.6715	77.5		−22.0		
	0.6736			0.6717	415.3		−21.3		
	0.6754								
	0.6771								
2	0.7339	1450							Lyα
	0.7423								
2	0.7613	920	1	0.7663	2375.7		−21.3		Lyα
	0.7667								
2	0.8294	2750							Lyα
	0.8463								
2	0.9653	1900							Lyα
	0.9778								
						3C 351			
?			2	0.0708	296.2	220×70	−20.0	140	OI geoc.
				0.0713	62.9		−18.0		
1			2	0.0860	325.3	200×160	−21.0	1650	Lyα
	0.0920			0.0910	125.3		−20.2		
?			4	0.0962	498.9	250×180	−22.4	380	C II Gal.
				0.0970	692.2		−19.1		
				0.0973	405.7		−22.3		
				0.0976	389.3		−20.5		
2	0.1611	1670	2	0.1621	722.4	170 ×90	−22.9	1570	Lyα
	0.1676			0.1682	143.8		−19.4		
2	0.2216	320	2	0.2217	710.6	1000×70	−19.5	1050	metal
	0.2229			0.2260	347.0		−19.8		and Lyα
3	0.3621	2080	2	0.3621	189.2	120×60	−21.5	1930	Lyα
	0.3646								and metal
	0.3716			0.3709	301.6		−23.7		
						H 1821+6419			
1	0.1806		2	0.1785	672.6	150 ×240	−21.0	2750	Lyα
				0.1894	952.4		−22.2		
1	0.2972		25	0.2844	56.6	3000×1000	−23.3	1100[a]	metal
				to	to		to		
				0.3040	1534.4		−20.7		

[a] This is the velocity dispersion of the cluster.

the two galaxies at the same redshift $z_g = 0.6716 = z_a$, although there is a rich clump of neighboring Lyα absorption lines and the two galaxies could alternatively be associated with different Lyα absorbers. There are two pairs of galaxies with impact parameters smaller than $1h_{50}^{-1}$ Mpc, but their velocity relative to the absorber is large (> 750 km s^{-1}), and thus they do not represent cases of Lyα absorber-galaxy associations.

To further study the presence of galaxy clustering in the quasar fields, we construct the galaxy surface-density map for the different fields. At each point, this density is calculated by summing the contribution of all the galaxies in the field. A two-dimensional Gaussian function is assigned to each galaxy. This Gaussian function is normalized and centred on the galaxy position. The field galaxy surface-density, averaged over the whole sky, to our limiting apparent magnitude $m_{r,lim} = 22.5$, $\langle\rho\rangle$, is derived by integrating the exponential law given by Le Brun et al. (1993) up to $m_{r,lim}$.

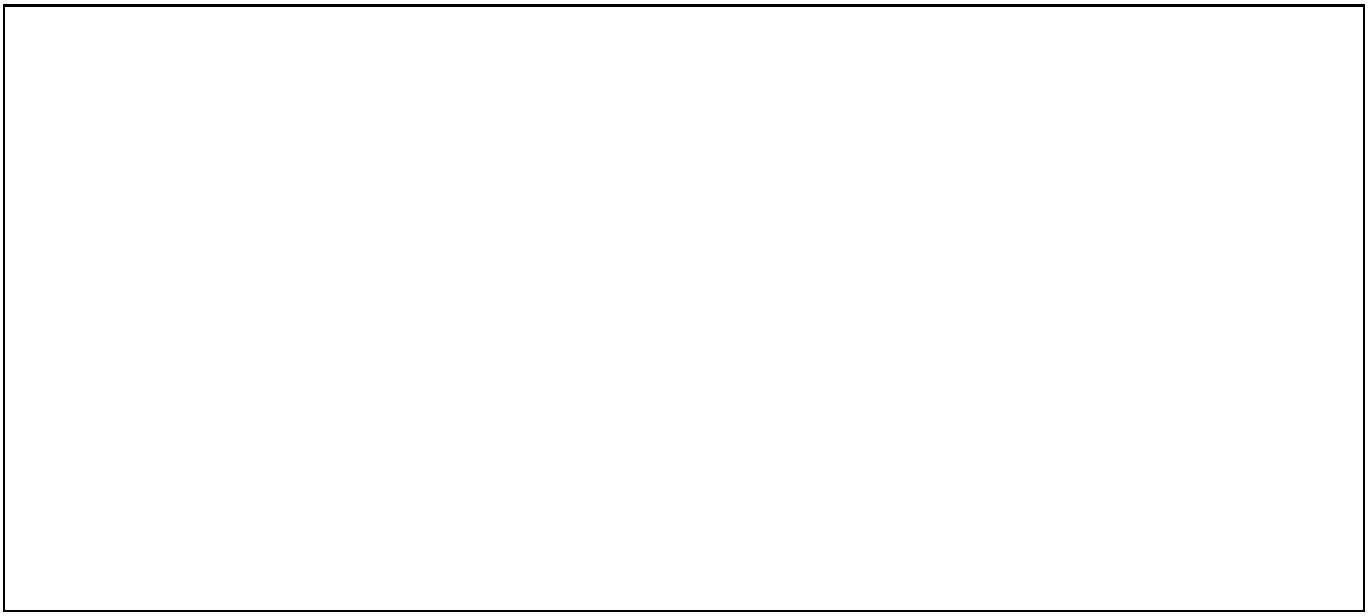

Fig. 9. Galaxy surface-density around TON 153.The full line is the mean density ρ_0, the dotted line is 1 σ below ρ_0, the short-dashed line is 1 σ above ρ_0 and the dot-dashed line is 2σ above ρ_0. The cross indicates the quasar location

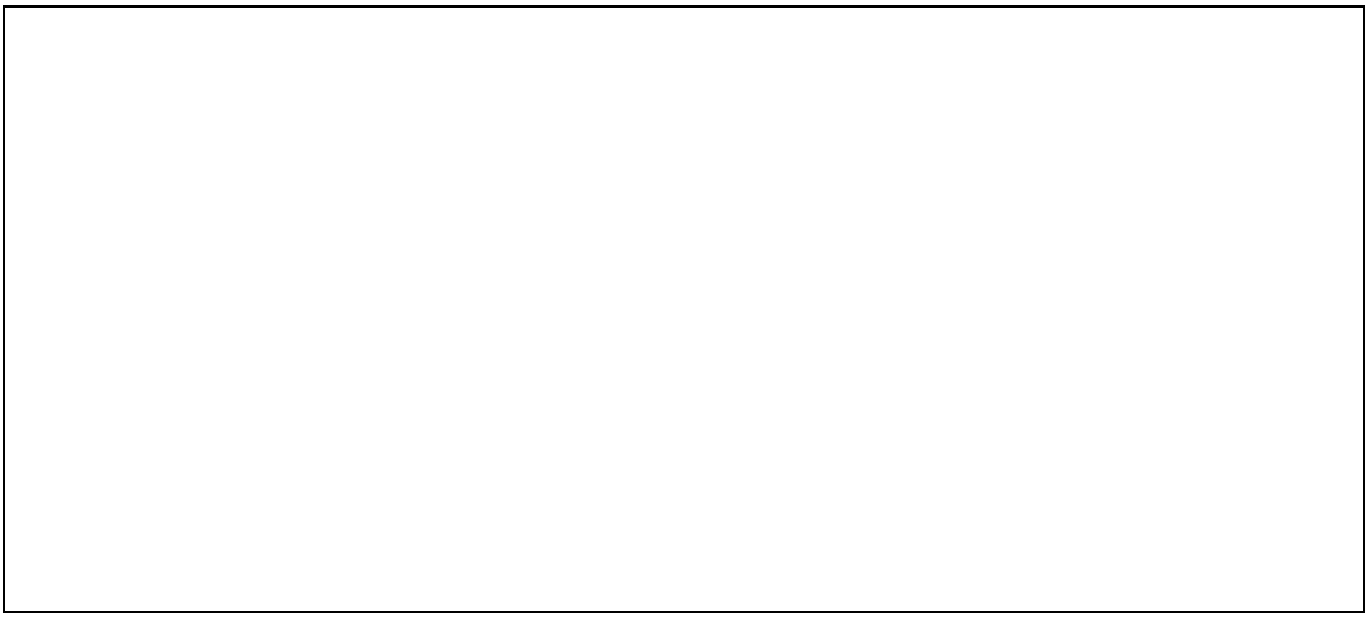

Fig. 10. Same as Fig. 9 for 3C 351

This leads to a characteristic, projected distance between galaxies $\langle d \rangle = \langle \rho \rangle^{-\frac{1}{2}}$, which is used as the HWHM of the Gaussian function. For each field, we then estimate the average galaxy surface-density for $m_{\rm r} \leq m_{\rm r,lim}$, ρ_0. In Figs. 9, 10 and 11, the isodensity contour at ρ_0 is plotted as a solid line. The standard deviation is

$$\sigma = \frac{\sqrt{n}}{s}, \tag{3}$$

where n is the average number of galaxies in a cell of size $2\langle d \rangle$, and s is the surface of such a cell. In the field of H 1821+6419, these quantities have been derived from an area which excludes the galaxy cluster, since it would otherwise lead to overestimating ρ_0. The contour levels are plotted as dotted lines for $\rho_0 - 1\sigma$, small-dashed lines for $\rho_0 + 1\sigma$, dot-dashed lines for $\rho_0 + 2\sigma$, and for the contours at 3σ and above as long-dashed lines. The only strong

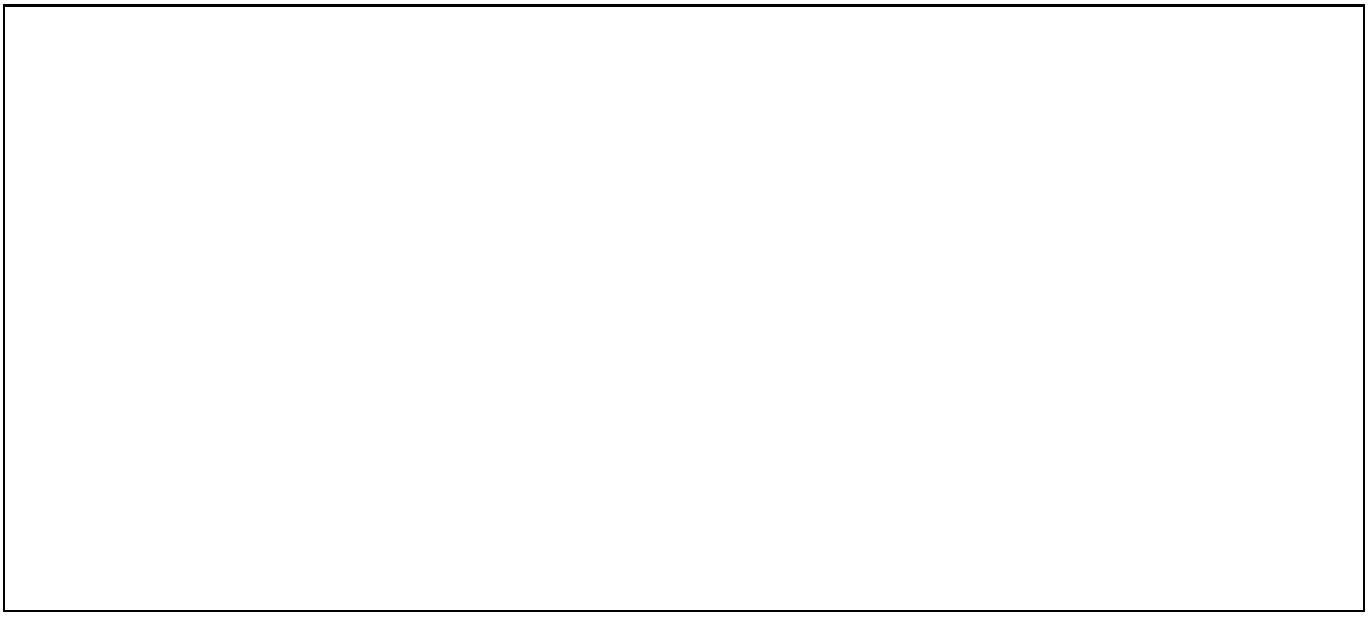

Fig. 11. Same as Fig. 9 for H 1821+6419, and long-dashed lines for 3 to 8 σ above ρ_0

feature appearing in these surface-density maps is the cluster at the redshift of the quasar H 1821+6419, which is a 8σ overdensity. There is no overdensity, even at the 2σ level, in the field of 3C 351, while there is a group west to the image of TON 153 detected at the 2σ level. This overdensity contains some galaxies at $z \simeq 0.67$. At this redshift, our magnitude limit corresponds to L* galaxies, and deeper imaging over a large field is needed to confirm this overdensity.

5. Conclusions

The present survey of galaxies in the fields around quasars at intermediate redshift, combined with previous similar studies, leads to a sample of 32 Lyα absorber-galaxy associations and 11 galaxies without associated Lyα absorption. The redshift coincidences for the associations is statistically significant. This survey favors the existence of two populations among the Lyα absorber-galaxy associations at $\langle z_{\rm a} \rangle \sim 0.32$ and have direct implications regarding the size of gaseous galactic halos. The continuity in impact parameters and H I column densities between metal-rich and Lyα-only absorber-galaxy associations suggests that the Lyα absorbers are part of coherent structures, and the results of the search for various correlations imply that only a limited fraction of these absorbers are physically associated with normal galaxies. Almost invisible galaxies with low surface brightness and smaller initial central column density of gas than ordinary galaxies could be responsible for a large fraction of Lyα absorbers (Salpeter & Hoffman 1995). This class of galaxies could reside in filaments which also contain some ordinary galaxies and galaxy groups.

The link with the large-scale structures of the universe is suggested by 1) the similarity between the narrow distribution of the relative velocity, $|\Delta v|$, of the Lyα absorber-galaxy associations (HWHM = 120 km s^{-1}) and the local thickness of large-scale structures, 2) the lack of correlation between the impact parameter of the galaxies and their luminosity or $|\Delta v|$, 3) the Lyα absorber-galaxy correlation function which is positive, although not as strong as the galaxy-galaxy correlation function on large scales (Morris at al. 1993). The small values of $|\Delta v|$ found recently by Dinshaw et al. (1995) for Lyα absorbers at intermediate redshift toward a close quasar-pair are similar to the HWHM of the relative velocity distribution of absorber-galaxy associations. As pointed out by these authors common Lyα absorptions detected in quasar-pairs do not allow to discriminate directly between single coherent clouds and correlated but distinct features. The dimensions inferred from these observations constrain either galactic halo sizes or correlation lengths within large-scale structures.

The gaseous galactic halos traced by Mg II and C IV absorptions have radii up to $\sim$ 75-95 h_{50}^{-1} kpc and they may extend further out, their most outer parts giving rise to only Lyα absorption. The overall size of these halos can be derived from the ratio of the cumulated number of Lyα absorber-galaxy associations for impact parameters smaller than D to the total number of galaxies with impact parameters $< D$, shown in Fig. 12. This fraction drops from unity at $D < 175 h_{50}^{-1}$ kpc down to about 0.65 for $D > 220 h_{50}^{-1}$ kpc and is then roughly constant up to the largest scales of our combined sample (1.8 h_{50}^{-1} Mpc). Our survey has substantially increased the number of Lyα absorber-

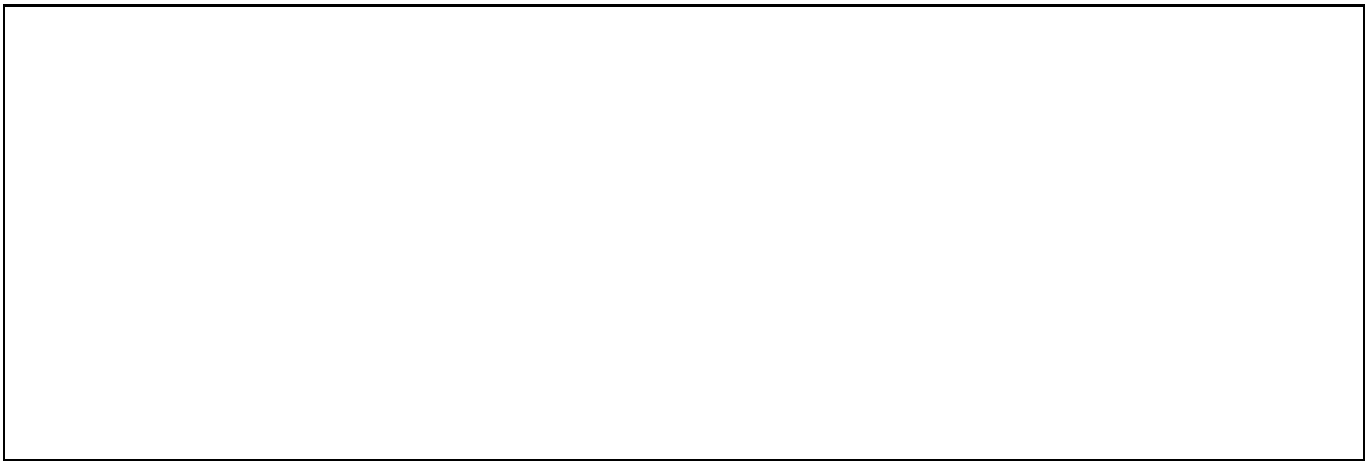

Fig. 12. Cumulated fraction of Lyα absorber-galaxy associations versus impact parameter

galaxy associations at intermediate and large impact parameters, and thus this break does not extend to as large impact parameters as found by LBTW. Our results then suggest that the characteristic dimensions implied by the observations of Dinshaw et al. (1995) are more indicative of correlation lengths than actual halo radii. The size of Lyα absorption-selected galactic halos of luminous field galaxies is about three times larger than the inner parts traced by Mg II absorption. Although large, this limited halo size as compared to the range of impact parameters investigated can account for the weak anti-correlation between D and $w_{\rm r}$ found for the sample of Lyα absorber-galaxy associations restricted to $w_{\rm r} \geq 0.24$ Å.

The presence of groups and clusters of galaxies can be investigated, even though our spectroscopic survey is incomplete. Indeed, clustering can be derived from galaxy density fluctuations within each field (see Sect. 4.4). The cluster of galaxies associated with the radio-quiet quasar H 1821+6419 is obviously present (see Fig. 11). There is a single absorption system at $z_{\rm a} \simeq z_{\rm e}$, and its ionization level is high. This absorber could then be associated to the quasar and its close environment rather than to the cluster itself. There is also possibly a group of galaxies west of the quasar TON 153 detected only at the 2σ level, which could be a geometrical superposition of sheets of large-scale structures at $z \simeq 0.660$ and 0.673. Since the average distance between galaxies within a sheet of large-scale structures is $\simeq 6h_{50}^{-1}$ Mpc (see e.g. Ramella et al. 1989, 1992), i.e. at least 1.5 times our field size (for $z_{\rm g} = z_{\rm a} \leq 0.7667$), the presence of two or more galaxies in one field with relative velocities smaller than 500 km s^{-1}would reveal the presence of at least a loose group. In our three fields, aside from an interactive galaxy-pair, there is no single Lyα absorption unambiguously associated with two or more galaxies. There are one pair and one group of galaxies spanning at most 380 km s^{-1}, but there is no available information on the associated Lyα absorption. The presence of Lyα absorbers in a rich galaxy environment is thus not likely, as already discussed by Morris et al. (1993). This question will be more firmly answered after completion of our survey.

References

Bahcall J.N., Jannuzi B.T., Schneider D.P., et al., 1991, ApJ 377, L5
Bahcall J.N., Jannuzi B.T., Schneider D.P., et al., 1992, ApJ 397, 68
Bahcall J.N., Bergeron J., Boksenberg A., et al., 1993, ApJS 87, 1
Bahcall J.N., Bergeron J., Boksenberg A., et al., 1994, ApJ, submitted
Bergeron J., Boissé P., 1991, A&A 243, 366
Bergeron J., Cristiani S., Shaver P.A., 1992, A&A 257, 417
Bergeron J., Petitjean P., Sargent W.L.W., et al., 1994, ApJ 436, 33
Cen R., Miralda-Escude J., Ostriker J.P., Rauch M., 1994, ApJ 437, L9
de Zeeuw T., Franx M. 1991, ARA&A 29, 239
Dinshaw N., Foltz C.B., Impey C.D., Weymann R.J., Morris S.L., 1995, Nature 373, 223
Heckman T.M., Armus L., Miley G.K., 1990, ApJS 74, 833
Isobe T., Feigelson E.D., Nelson P.L., 1986, ApJ 306, 490
Lanzetta K.M., Bowen D.V., Tytler D., Webb J.K., 1995, ApJ 442, 538 (LBTW)
LaValley M., Isobe T., Feigelson E.D., 1992, BAAS 24, 839
Le Brun V., Bergeron J., Boissé P., Christian C., 1993, A&A 279,33
Lu L., Savage B.D., 1993, ApJ 403, 127

Morris S.L., Weymann R.J., Dressler A., et al., 1993, ApJ 419, 524
Morris S.L., van den Bergh S., 1994, ApJ 427, 696
Petitjean P., Mücket J.P., Kates R.E., 1995, A&A 295, L9
Ramella M., Geller M.J., Huchra J.P., et al., 1989, ApJ 344, 57
Ramella M., Geller M.J., Huchra J.P., et al., 1992, ApJ 384, 396
Rubin V.C., Thonnard N., Word W.K. Jr., 1982, AJ 87, 477
Schneider D.P., Bahcall J.N., Gunn J.E., Dressler A., 1992, AJ 103, 1047
Salpeter E.E., Hoffman G.L., 1995, ApJ 441, 51
Steidel C.C., 1993, The Properties of Absorption-Line Selected High-Redshift Galaxies. In Schull, J.M., Thronson, H.A. Jr (eds.) The Environment and Evolution of Galaxies. Kluwer, Dordrecht, p. 263
Stocke J.T., Shull J.M., Penton S., Donahue M.E., Carilli C., 1995, preprint
Tytler D.A., Sandoval J., Fan X.-M., 1993, ApJ 405, 57

This article was processed by the author using Springer-Verlag LaTeX A&A style file *L-AA* version 3.